

International Journal of Modern Physics E
© World Scientific Publishing Company

Strangeness production in Au+Au reactions at $\sqrt{s_{NN}} = 62.4$ GeV*

Ionut-Cristian Arsene^{1,2} for the BRAHMS Collaboration

¹*Physics Department, University of Oslo,*

P.O.Box 1048 Blindern, N-0316 Oslo, Norway;

²*Institute for Space Sciences, Bucharest-Magurele, Romania.*

i.c.arsene@fys.uio.no

Received (received date)

Revised (revised date)

The measurement of strangeness is a valuable tool for understanding the reaction mechanism of nuclear collisions since all the strange particles need to be created during the reaction. Also, strangeness enhancement is one of the predicted signals of the QGP. In the present work we will discuss the behaviour of the strangeness production (i.e. K/π ratio) with rapidity and baryo-chemical potential in Au+Au collisions at 62.4 AGeV. In this particular reaction, BRAHMS is able to identify particles over 3.5 rapidity units and thereby cover a wide range of \bar{p}/p ratios, including the fragmentation region. We will show spectra and ratios of identified particles as a function of p_T and rapidity.

1. Introduction

One of the first proposed signals of quark gluon plasma (QGP) is strangeness enhancement because the mass of strange quarks and anti-quarks is of the same magnitude as the temperature at which the hadrons are expected to dissolve into quarks.¹ Thus, the abundance of these quarks is particularly sensitive to the conditions and dynamics of the deconfined-matter phase.

Going from energies as low as $\sqrt{s_{NN}} = 1$ GeV up to the top SPS energies, the strangeness production (e.g. well approximated by the K^+/π^+ ratio) increased sharply and reached a maximum.² Continuing at higher energies towards RHIC, the K^+/π^+ ratio started to decrease and has a tendency to level off around ≈ 0.15 . This kind of behaviour suggested some sort of a transition to a new regime.

In the present work, we will discuss the behaviour of the strangeness production with rapidity in the Au+Au collisions at $\sqrt{s_{NN}} = 62.4$ GeV measured by the BRAHMS experiment. In this particular reaction, BRAHMS is able to identify particles up to about 3.5 units of rapidity, including the collision fragmentation region.

*Proceeding for the poster contribution at The 19th International Conference on Ultra-Relativistic Nucleus-Nucleus Collisions.

2 *I.C. Arsene for BRAHMS Collaboration*

2. Experimental setup

BRAHMS is one of the four experiments which were taking data at the Relativistic Heavy Ion Collider (RHIC).³ The setup of the experiment includes two spectrometer arms, allowing for a very good precision in momenta and particle identification measurements over a wide rapidity region. The mid-rapidity arm is capable of separating π , K , p and \bar{p} particles up to 2.5 GeV/c while the forward arm can identify particles up to 35-40 GeV/c by using a Cherenkov ring detector. Both arms cover a very small solid angle but they can be moved around the interaction point to measure particles from 90° (mid-rapidity) up to 2.3° (the most forward rapidity). Also, by varying the field in the spectrometer magnets, BRAHMS is able to sweep different momenta intervals. In order to distinguish the centrality class of the events, BRAHMS is using a Multiplicity Array detector composed of scintillator tiles and silicon strip detectors. This array has a cylindrical geometry and is located around the nominal interaction point.

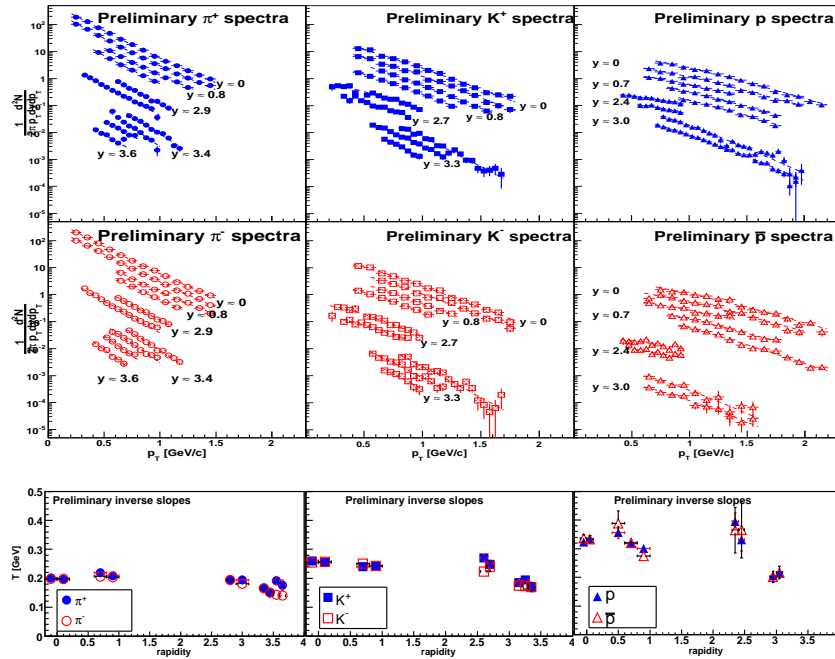


Fig. 1. Top two rows: Identified particle spectra from 0-10% central Au+Au collisions at $\sqrt{s_{NN}} = 62.4$ GeV in different rapidity slices. All the spectra are fitted by m_T exponentials. Bottom row: Inverse slope parameters versus rapidity obtained by fitting the p_T spectra shown in the top two rows with exponentials in m_T . The error bars shown are statistical only.

3. Data analysis

We analyzed data from the 4-th year of running at RHIC when a relatively small dataset was collected for the Au+Au collisions at $\sqrt{s_{NN}} = 62.4$ GeV. For this work we used data from both BRAHMS spectrometer arms. The particle identification was done by using time of flight detectors for relatively low momenta and the RICH detector to extend the particle identification in high field settings. We do not want to go into a detailed description of the experimental data processing, but one can find more informations in these references.^{4,5}

4. Results and discussions

In Fig. 1 we show the p_T spectra for π^\pm , K^\pm , \bar{p} and p obtained from the 10% most central events in different slices of rapidity, ranging from zero up to rapidity 3.7 in the case of pions. The spectra were corrected for in-flight decays, multiple scattering and hadronic absorption (in the case of anti-protons).

The spectrum was fitted with an exponential function in m_T having the form $f(m_T) = k \exp(-m_T/T)$. T is a fit parameter and is often called the inverse slope parameter or effective temperature. These fitted temperatures (see Fig. 1 bottom row) are different for different particle species and their values are sensibly higher than the ones calculated at kinetic freeze-out with different statistical models.⁷ The slopes reflect the mechanisms involved in the particle production, the time evolution of the fireball, and the apparent disagreement with statistical models values reflect non-thermal effects like flow, resonance decays, etc. In Fig. 1 we show the distribution of effective temperatures versus rapidity for all identified particles. You can see there that higher masses particles have higher slope parameters mainly due to flow, but there is also a slight decrease of temperatures at high rapidities.

By integrating the fitting functions over the entire transverse momenta range, we can obtain the dN/dy yields (see Fig. 2). The proton and anti-proton yields are not shown here but they can be found in reference⁷. This procedure involves a degree of extrapolation mainly due to low p_T particles falling outside our acceptance. The errors shown in the figure are statistical only. The dN/dy distributions versus rapidity have gaussian shapes for all identified particles except for protons which peak at forward rapidity.

In Fig. 3 we plotted the anti-particle to particle ratios versus rapidity together with the same ratios obtained from the Au+Au at $\sqrt{s_{NN}} = 200$ GeV.⁶ At both energies, we observe that pion ratios and to some extent kaon ratios approach unity around mid-rapidity suggesting that the particle production in the central region is dominated by pair creation. This is not the case for protons. We also clearly see that the kaon and proton ratios at the lower energy are smaller compared to the ones at full RHIC energy. This can be explained by the higher net-proton densities present in the 62.4 GeV collisions at mid-rapidity.

Of particular interest for this work is the \bar{p}/p ratio which is related to the baryo-chemical potential. For the 62.4 GeV collisions this ratio varies from ≈ 0.45

4 *I.C. Arsene for BRAHMS Collaboration*

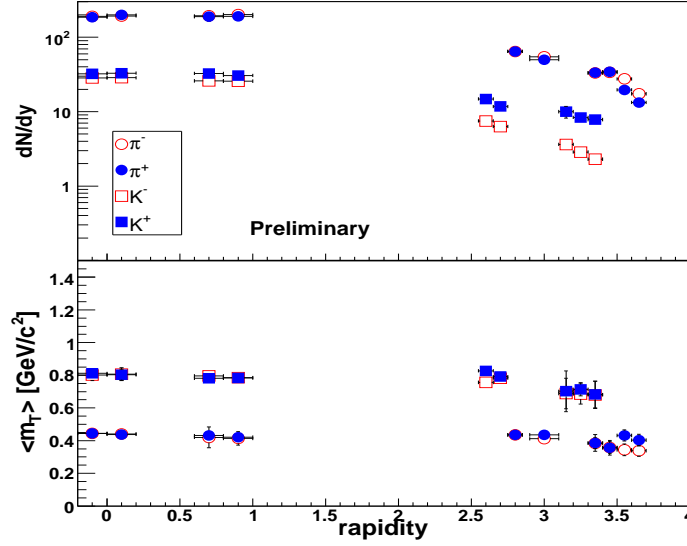


Fig. 2. Top panel: dN/dy yields as a function of rapidity for π^\pm and K^\pm in the 0-10% central Au+Au collisions. The yields are obtained by fitting the spectra with m_T exponentials and extrapolating on the entire m_T range. Pions are denoted by circles while kaons by squares. The open symbols are for negative particles and filled symbols for the positives. Bottom panel: Average transverse mass as a function of rapidity. The error bars are statistical only.

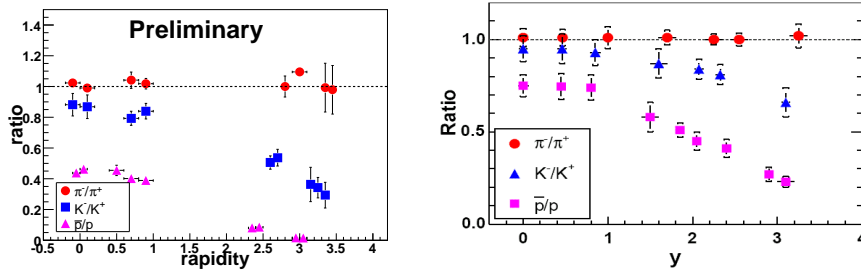


Fig. 3. Left panel: Anti-particle/particle ratios in Au+Au collisions at $\sqrt{s_{NN}} = 62.4\text{GeV}$. The errors are statistical only. Right panel: the same ratios at $\sqrt{s_{NN}} = 200\text{GeV}$.⁷

at mid-rapidity to ≈ 0.015 at rapidity 3. The very small values reached are in the same range as the ones obtained at SPS energies at mid-rapidity, making thus possible a comparison between the two systems.

In Fig. 4 on the left panel we show the K^\pm/π^\pm ratios versus rapidity for the 62.4 AGeV Au+Au collisions while in the right panels we show a dependence of these ratios measured at mid-rapidity on center of mass energy. At high rapidity, inside

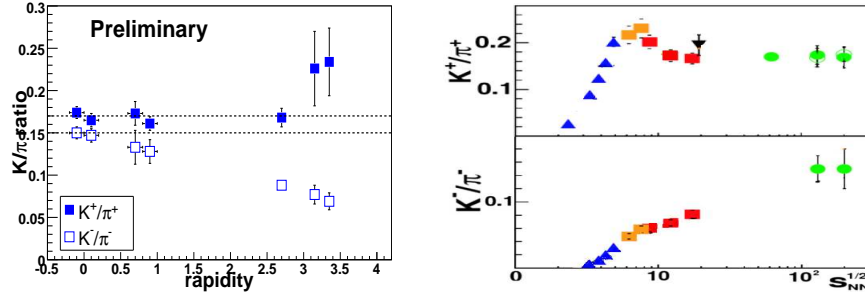
Strangeness production in Au+Au reactions at $\sqrt{s_{NN}} = 62.4$ GeV 5

Fig. 4. Left panel: K^+/π^+ and K^-/π^- ratios versus rapidity in Au+Au collisions at $\sqrt{s_{NN}} = 62.4$ GeV. The filled symbols denote the positive ratio and open ones the negative ratio. The error bars are statistical only. Right panels: Mid-rapidity K^+/π^+ and K^-/π^- ratios versus c.m. energy. The triangles are for the AGS data, the squares for SPS and circles for RHIC.²

the fragmentation region, we observe a splitting between the positive and negative K/π ratios. The same splitting was observed in the 200 AGeV data as well on a smaller scale.⁶

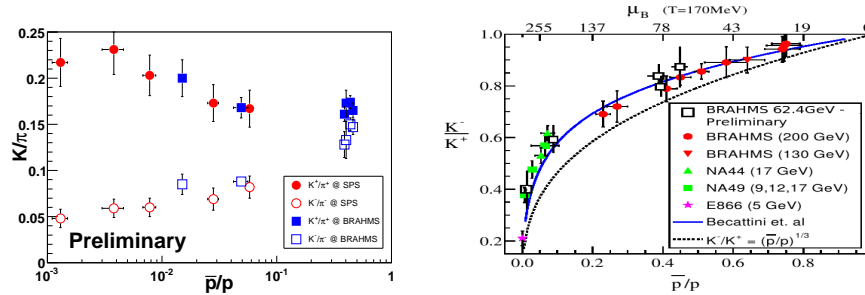


Fig. 5. Left panel: K/π ratios versus \bar{p}/p ratio from 0-10% Au+Au collisions at $\sqrt{s_{NN}} = 62.4$ GeV in different rapidity intervals and from SPS energy Pb+Pb collisions at mid-rapidity.⁹ The squares stand for BRAHMS points while circles stand for SPS results. The errors on the BRAHMS points are statistical only. The errors for the SPS points contain both statistical and systematic errors. Right panel: K^-/K^+ versus \bar{p}/p ratio. The blue solid line is a statistical model calculation with a chemical freeze-out temperature fixed to 170 MeV. The dashed line corresponds to $K^-/K^+ = (\bar{p}/p)^{1/3}$ where the strange quark chemical potential is taken to be zero.^{6,7}

In Fig. 5 (left panel) we show the dependence of K/π ratios on the \bar{p}/p ratio in several rapidity slices for the Au+Au collisions at $\sqrt{s_{NN}} = 62.4$ GeV and in mid-rapidity for different Pb+Pb SPS collision energies. We observe that the RHIC points agree with the SPS results in the same baryo-chemical range. This suggests that the local system formed at high rapidity in 62.4 GeV collisions is chemically equivalent with the systems formed at SPS mid-rapidity.

6 *I.C. Arsene for BRAHMS Collaboration*

Furthermore, in the right panel we show the $\sqrt{s_{NN}}$ dependence of K^-/K^+ ratio on the \bar{p}/p ratio using data from energies ranging from the E866 experiment ($\sqrt{s_{NN}} = 5\text{GeV}$) to the top RHIC energy. All these points are very nicely fitted by a statistical model calculation with a chemical freeze-out temperature fixed to 170 MeV but letting the baryon potential to vary.^{7,8}

5. Conclusions

We showed results on identified particles obtained with the BRAHMS detector in Au+Au collisions at $\sqrt{s_{NN}} = 62.4\text{ GeV}$. At mid-rapidity, the anti-particle to particle ratios are lower than the ones obtained at top RHIC energy. The anti-proton/proton ratio shows a steep decrease with rapidity, reaching values similar to the ones obtained at SPS. Our K^+/π^+ and K^-/π^- ratios at forward rapidity show the same dependence on the \bar{p}/p ratio as the corresponding midrapidity ratios at the SPS. A similar scaling is observed for the K^-/K^+ ratio.

References

1. J. Rafelski and R. Hagedorn, *Statistical mechanics of quarks and hadrons*, North Holland, Amsterdam, 1981, p. 253.
2. NA49 Collaboration, *J.Phys.G:Nucl.Part.Phys.* **32** (2006) S43-S50.
3. M. Adamczyk *et al*, BRAHMS Collaboration, *Nucl.Inst.Meth.* **A499** (2003) 437.
4. P. Christiansen, Ph.D. Thesis, Copenhagen University, Denmark, 2003.
5. D. Ouerdane, Ph.D. Thesis, Copenhagen University, Denmark, 2003.
6. I. Arsene *et al.*, BRAHMS Collaboration, *Nucl.Phys.* **A757** (2005) 1, nucl-ex/0410020
7. I.G. Bearden *et al.*, BRAHMS Collaboration, *Phys.Rev.Lett.* **90** (2003) 102301 and references therein
8. F.Becattini *et al.*, *Phys.Rev.* **C64** (2001) 024901
9. NA49 Collaboration, *Phys.Rev.* **C73** (2006) 044910
10. I.Arsene *et al.*, BRAHMS Collaboration, *J.Phys.* **G30** (2004) S667
11. H.H.Dalsgaard for the BRAHMS Collaboration, *in these proceedings*